Fast Ignition without Hole Boring

S. Hain and P. Mulser

Theoretical Quantum Electronics (TQE), Darmstadt University of Technology, Hochschulstrasse 4A, D-64289 Darmstadt, Germany

(Received 31 August 2000)

A fast-ignitor scheme for inertial confinement fusion is proposed which works without hole boring. It is shown that a thermonuclear burn wave starts from the pellet corona when an adequate amount of energy (typically 10 kJ) is deposited in the critical layer by a petawatt laser ("coronal ignition"). Burn efficiencies as high as predicted for standard central spark ignition are achieved. In addition, the scheme is surprisingly insensitive to large deviations from spherical precompression symmetry. It may open a new prospect for direct drive.

DOI: 10.1103/PhysRevLett.86.1015 PACS numbers: 52.57.–z, 28.52.–s, 52.38.–r, 52.50.Jm

The concept of fast ignition of precompressed deuterium-tritium (DT) pellets, proposed by Tabak in 1994 [1], has opened new possibilities in the field of inertial confinement fusion (ICF) with lasers and heavy ion beams. The standard scheme so far provides compression of the fuel pellet and its precisely timed ignition by a central spark from a converging shock with the aid of one single driver [2]; it poses severe restrictions on the quality of drivers and the conception of pellets for ICF [3].

The idea of fast ignition consists of separating compression from ignition. First, a capsule is imploded to several thousands of solid density by a powerful driver in the conventional approach; second, a hole is bored through the low and medium density ablative corona by a superintense laser of $10^{18}-10^{20}$ W cm^{-2} intensity to bring the critical density as close as possible to the high density core of the capsule; third, core ignition is achieved by a jet of fast electrons which are generated by the highest intensity portion of the hole boring laser pulse or by a separate, more intense light pulse. Despite the striking advantages of the new scheme (pellet compression, unstable modes, and preheat less critical), its design in detail has little progressed during recent years. Fast ignition studies performed so far have mainly concentrated on the energy to initiate burn when deposited in a suitable region of the pellet [4]. For the rest, the concept of central ignition and the necessity of hole boring are considered as essential elements of the scheme [5,6].

In our recent studies of fast ignition we found that hole boring, with the aim of bringing the laser-plasma coupling layer close to the compressed high density core, does not work as expected. The ponderomotive pressure mainly causes a drastic deformation of the critical surface. This is a very positive effect because it leads to a remarkable increase of absorption [7]. Therefore, based on the new idea of asymmetric ignition, we propose an alternative fast ignitor scheme which works without hole boring: deposition of the laser energy of a single unshaped pulse in the corona of the precompressed pellet and ignition of a burn wave propagating from the deposition region through the fuel. We show that this scheme of coronal ignition is (i) as efficient as standard central spark ignition and, furthermore, is (ii) widely insensitive to mass distribution asymmetries of the precompressed pellet.

To prove this we performed burn simulations in cylindrical geometry (coordinates x, r) by the use of a 2D Yabe-type hydrocode [8] which incorporates electronic heat conduction (flux-limited Spitzer), diffusive mass and energy transport of α particles (Atzeni-Caruso model [4,9]) and volume emission of Bremsstrahlung. The laser energy is either directly deposited at the critical surface (use of Lambert-Beer's law, 100 keV hot spot generation, energy transport by an electronic heat wave [10]) or converted at the critical surface into a collimated beam of fast electrons which subsequently deposit their energy in the plasma (ballistic model, use of a Bethe-like energy loss formula [11], including a self-consistent electric field which drives the return current, in analogy to [12]). There are indications for the formation of collimated beams of relativistic electrons under certain conditions in experiments [13] and simulations [7,14,15] and their breaking up into numerous filaments [7,14,16]. At present, neither merging into a single beam ("superchannel") nor splitting into filaments is understood. Finally, nuclear burn is calculated in a three-temperature model for electrons, ions, and α particles. In addition to the energy flux of the α particles, their mass flux is also taken into account. The system of conservation equations is presented in [10]. The electron fluid is heated by the laser. From there the energy flows into the ions. This imposes a limit on the laser pulse length of a few tens of ps. With much longer deposition times a part of the energy is dispersed in hydrodynamic expansion. The burn front is triggered by the energy diffusion processes. When inertia effects dominate, the compression front decouples from the electron heat front and ignition fails (Fig. 1): The thermal wave has to overlap with the shock to support it (compression $\kappa \simeq 1.5$).

The numerical simulations, based on this model, were performed with pellets of about 2 mg mass and peak densities ranging from 300 to 500 g cm^{-3} and deposited energies up to several tens of kJ. For ignition to be

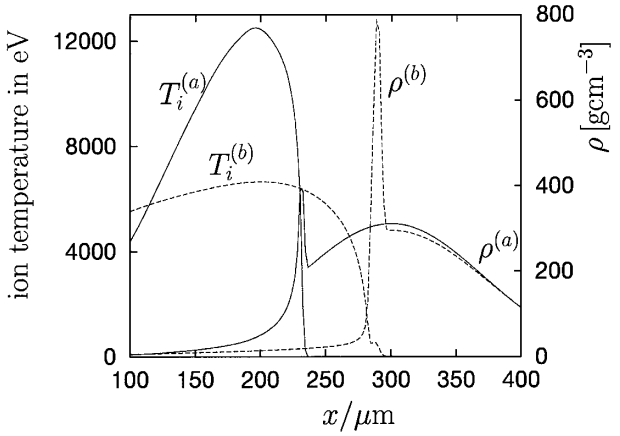

FIG. 1. Ion temperature and mass density profiles on the axis $r = 0$ from 2D burn simulations; parameters: pellet mass 1.7 mg, peak density $\rho_{\mathrm{DT}} = 311\ \mathrm{g\,cm^{-3}}$, characteristic length of density profile $L = 100\ \mu$m, pulse duration $\tau = 20$ ps (*a*),(*b*), laser intensity $I = 1.2 \times 10^{20}\ \mathrm{W\,cm^{-2}}$ (*a*), and $I = 0.8 \times 10^{20}\ \mathrm{W\,cm^{-2}}$ (*b*). The profiles are taken after $t = 44$ ps (*a*) and $t = 104$ ps (*b*). While case (*a*) shows a propagating burn front (moderate shock compression $\kappa < 2$), in case (*b*), dashed lines, the compression front decouples from the heat front and ignition fails (strong shock, $\kappa > 2$).

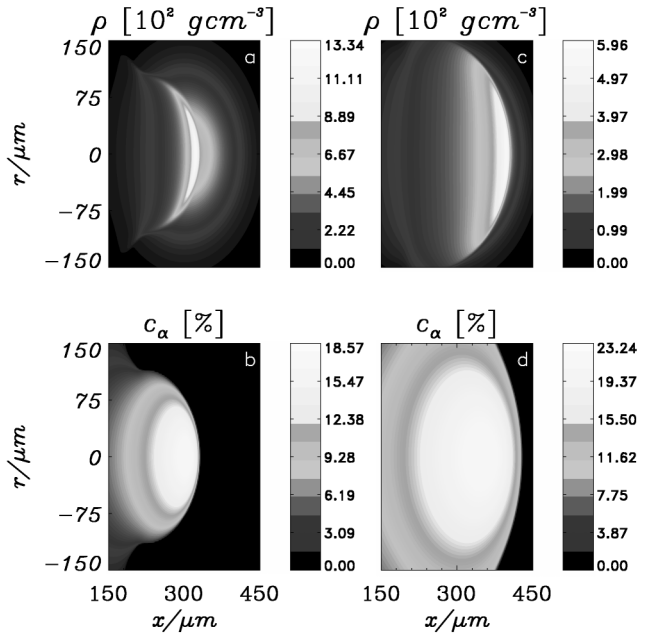

FIG. 2. Burn of a laser-ignited precompressed DT pellet, illustrated by the contour plots of the mass density ρ and the α-particle concentration c_α at $t = 62$ ps (a,b) and $t = 77$ ps (c,d). In (a) the burn wave just crosses the dense core. Parameters: mass $M_{\mathrm{DT}} = 2.9$ mg, Gaussian density profile with peak density $\rho_{\mathrm{DT}} = 519\ \mathrm{g\,cm^{-3}}$, and profile length $L = 100\ \mu$m. Initial condition: spherical implosion, linear velocity profile with $v = 3 \times 10^7\ \mathrm{cm\,s^{-1}}$ radially inward at a distance of 100 μm from the center; laser intensity $I = 1.2 \times 10^{20}\ \mathrm{W\,cm^{-2}}$, pulse duration $\tau = 20$ ps, deposited energy $E = 9.0$ kJ. Igniting laser pulse comes from the left-hand side; ignition is initiated by the heat wave propagating inward. Burn fraction $\phi = 16.9\%$.

successful, laser intensities above $10^{20}\ \mathrm{W\,cm^{-2}}$ had to be chosen in all of our numerical runs. In a first example we show that the scheme works and what burn efficiencies can be expected. In Fig. 2 a case study is presented with a pulse energy $E = 0.934 I R^2 \tau = 9.0$ kJ ($R = 20\ \mu$m beam radius, $\tau = 20$ ps pulse duration) deposited at the edge of a precompressed pellet, $\langle \rho r \rangle = \int \rho\, dr = 4.6\ \mathrm{g\,cm^{-2}}$, peak fuel compression 2.6×10^3. In order to simulate a pellet which is still spherically imploding at the onset of the laser pulse, a radial flow velocity $v_r = -3 \times 10^7\ \mathrm{cm\,s^{-1}} \times r/100\ \mu$m (spherical coordinate r) is imposed. This value has been chosen in accordance with [3]. The burn fraction achieved is as large as $\phi = 16.9\%$. For a stagnating pellet ($v_r = 0$) it reduces to $\phi = 9.0\%$, which is still large. In both cases a heat wave with an electron temperature of several 10 keV starts from a 120 keV hot spot at the periphery of the pellet and propagates into the dense plasma where it initiates fuel burn. Since energy transport by fast electrons is highly directional at low densities [7,14], during laser energy deposition we use, for densities $\rho < \rho^* = 50\ \mathrm{g\,cm^{-3}}$, an anisotropic heat conduction model ($q_r < q_x$) according to $q_r = f q_x$, $f = 1 - \frac{I}{I_0}[1 - \tanh(\rho/\rho^*)]$. For high mass densities ρ, the transport becomes more and more isotropic and purely diffusive. In any case, whether $f < 1$ or $f = 1$ is set, the numerical results do not change significantly.

Alternatively, to achieve ignition in the ballistic deposition model [11], one needs laser intensities which are larger by a factor $\gtrsim$2, and peak densities of the compressed fuel which are higher by a factor $\sim$1.5 than in the purely diffusive transport model. This is due to the large range of relativistic electrons. In addition, we realized that the diameter of the fast electron beam must not be too small ($R \gtrsim 30\ \mu$m). As a consequence, the energy requirements become more stringent: The pulse energy needed to initiate self-sustained burn rises from 10 kJ to the order of 100 kJ.

To obtain a measure for the efficiency of coronal ignition its burn fraction ϕ is compared with ϕ from optimum central spark ignition of the standard model, under otherwise identical conditions. The criterion for central spark ignition is $(pr)_{\mathrm{s}} \leq 15\ \mathrm{Tbar}\mu\mathrm{m}$, p_{s} spark pressure, and r_{s} spark radius [17]. With the values $\rho_{DT} = 300\ \mathrm{g\,cm^{-3}}$, $kT_{\mathrm{s}} = 15$ keV, $r_{\mathrm{s}} = 15\ \mu$m, one obtains $(pr)_{\mathrm{s}} = 52\ \mathrm{Tbar}\mu\mathrm{m}$ and hence the criterion is fulfilled. However, in this isochoric configuration, ignition fails because the high pressure at the center creates a too violent shock moving radially outward and disassembling the pellet. Central spark ignition is accomplished by a shock converging towards lower density in the pellet center. Therefore, we lowered the density at the center by a factor $\xi = 5$–10 and increased the temperature T_{s} by ξ in order to create an isobaric condition [17]. A couple of computer runs showed that in a range of $\xi = 5$–10, ϕ depends only weakly on ξ ($\delta\phi \simeq 0.5\%$) which indicates that for central ignition we are close to an optimum of ϕ. For the imploding pellet of Fig. 2, with $kT_{\mathrm{s}} = 10 \times 15$ keV

we obtain $\phi_{\text{central}} = 16.5\%$ against $\phi_{\text{coronal}} = 16.9\%$. Surprising enough, coronal ignition can lead to equal burn performance and hence to equal gain as the standard model. At high peak densities (e.g. $\rho_{\text{DT}} = 500\ \text{g cm}^{-3}$) ignition is already achievable for $\xi = 1$. In general, with $\xi > 1$ the final burn fraction ϕ increases. For stagnating pellets, with $\rho_{\text{DT}} \simeq 300\ \text{g cm}^{-3}$ and coronal ignition, the typical burn fractions from simulations are $\phi \simeq 5\%-6\%$, compared with $\phi \simeq 7-9\%$ in central ignition. The latter values agree with estimates based on Ref. [3]. In coronal ignition the burn fraction can be slightly increased, i.e., by approximately 1%, if two opposite laser beams are used. The effect remains modest owing to cold fuel expulsion by the two colliding burn fronts. Nevertheless, the result shows that it is worth studying different ignitor configurations.

Conventional ignition is very sensitive to asymmetries. To study the response of coronal ignition to aspherical compression we shifted the center of mass of the compressed pellet along the axis of rotational symmetry, with direct energy deposition at the critical surface and pellet mass fixed (Fig. 3). This lead to a surprising result: $\phi = 6.5\%$ with symmetric pellet, and $\phi = 6.0\%$ and $\phi = 5.4\%$ with compression maximum shifted by 0.6 r_c away from and towards the laser beam, respectively (r_c critical radius). A shift to the right in Fig. 3 is less detrimental because the diffusion processes prevail over the inertia effects and the deflagration wave propagates faster over the cold fuel ("bush fire" effect), whereas, in the opposite case, cold fuel is partially pushed forward by the burn pressure acting like a snowplow. Furthermore, simulations suggest that external ignition favors soft compression profiles (e.g., Gaussian, with a characteristic density scale length of $L \sim 100\ \mu\text{m}$) rather than homogeneous hard cores ($L \sim 20\ \mu\text{m}$). This should not be surprising because in the latter case the danger of spark expulsion into the corona by the reactive high fuel pressure is enhanced. However, once ignited, homogeneous hard cores show, by 2%–3%, higher burn fractions.

Finally, we must explain why in the simulations presented no density channel forms which brings the laser coupling layer close to the dense core. In Fig. 4 the position of the laser piston (critical point x_c) is shown as a function of time for six runs. After 10–20 ps, hole boring stops and the laser piston is pushed back into the corona. Such behavior is expected also from basic analytical considerations. Under quasisteady conditions the energy balance for the absorbed laser intensity can be shown to be given by $4.6\rho_c s^3 = I - S$ [18], when completed by a diffusive or ballistic electron energy flow density S; ρ_c critical density, s sound speed. If one does not like to be faced with MeV temperatures, $I - S \simeq 0$ must hold. The ablation pressure is $P_a \simeq 2\rho_c s^2 + p_L$,

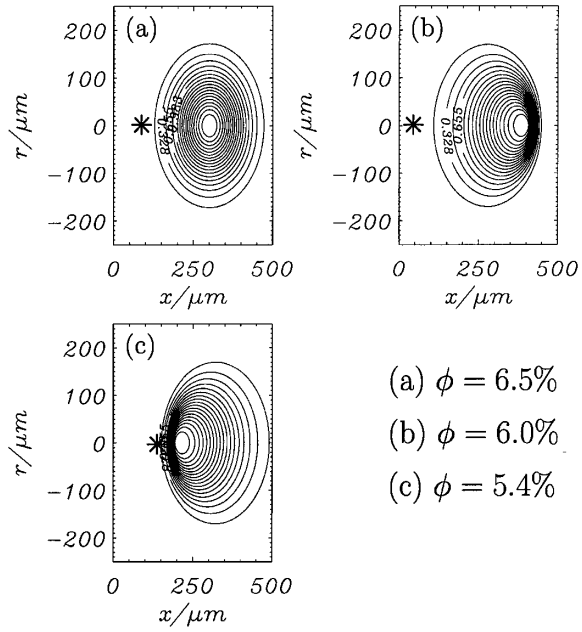

FIG. 3. Contour plots of different pellet mass distributions: (a) symmetric configuration, (b,c) asymmetric configurations with center of mass shifted along the axis to the right and to the left, respectively; pellet mass $M_{\text{DT}} = 1.7$ mg and peak density $\rho_{\text{DT}} = 311\ \text{g cm}^{-3}$ in all cases; scale lengths $L = 100\ \mu$m (a), $L_{\text{max}} = 160\ \mu$m, $L_{\text{min}} = 40\ \mu$m (b,c). Ignition is triggered by a laser pulse incident from the left-hand-side of intensity $1.2 \times 10^{20}\ \text{W cm}^{-2}$, pulse duration $\tau = 40$ ps, and pulse energy 18 kJ. Burn fractions ϕ refer to stagnating pellets. During ignition the laser energy deposition layer stays at the periphery; its initial position is marked by an asterisk.

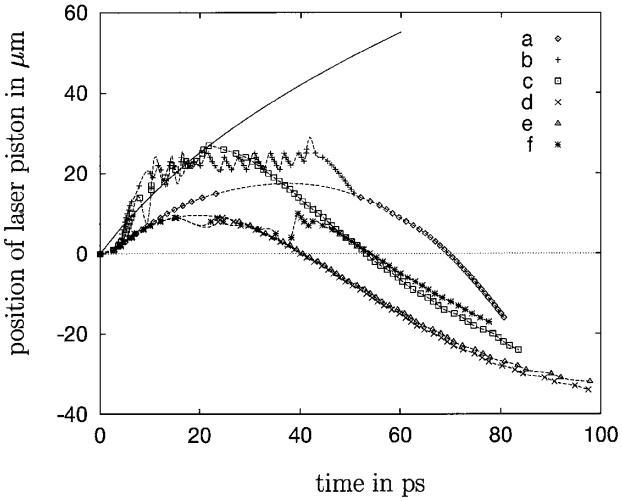

FIG. 4. Trajectories of the critical point x_c (position of the laser piston) of the pellet from Fig. 3(a) on the beam axis for different energy deposition models and laser pulse durations τ (smoothed rectangular pulse shapes). (*a*) Energy deposition by a collimated beam of fast electrons, $I = 4 \times 10^{20}\ \text{W cm}^{-2}$, $\tau = 50$ ps; (*b–f*) $I = 1.2 \times 10^{20}\ \text{W cm}^{-2}$; (*b,c*) anisotropic diffusion model (see text): (*b*) $\tau = 40$ ps, (*c*) $\tau = 20$ ps; (*d–f*) isotropic diffusive energy transport throughout the whole pellet: (*d,e*) $\tau = 20$ ps, (*f*) $\tau = 40$ ps. In all cases the motion of the laser piston stagnates at low densities $\rho_0 < 10\ \text{g cm}^{-3}$ and small perforation depths $h < 25\ \mu$m before the end of the pulse. For times $t > \tau$ the critical surface moves back into the corona. The solid curve is the numerical integration of $\dot{x} = [2I/\rho_0(x)c]^{1/2}$ (infinite pulse duration).

$p_L = (1 + \mathcal{R})I/(1 - \mathcal{R})c$, $\mathcal{R}$ reflection coefficient. Thus, $P_a = 0.7\rho_c^{1/3}(I - S)^{2/3} + p_L \simeq p_L$. The speed of matter perforation is given by the velocity v_S of the shock running into the undisturbed material of density ρ_0. Taking lateral expulsion of matter into account, $P_a = \rho_0 v_S^2/2$ holds [11]. The depth h of the hole as a function of time is the solution of the relation $\dot{h} = v_S$. For an exponential density profile $\rho_0(x) = \rho_c e^{x/L}$, with $\rho_c = 2.5 m_H \times 10^{21}$ cm^{-3}, $L = 26$ μm, one obtains $h = 166$ μm and $\rho_0(h) = 2.4$ g cm^{-3} for the parameters $I = 10^{20}$ W cm^{-2}, $\tau = 30$ ps. Thus, within the time window available (duration of the stagnation phase of the imploded pellet) a channel just up to typically solid density, far from 400 g cm^{-3} at 2×10^3 compression, has been achieved in the most favorable case.

A different consideration holds if the shock is preceded by a heat wave precursor, a situation which is favorable to ignition (see Fig. 1). A numerical solution of the nonlinear heat equation $\partial_t T = a\partial_x(T^{5/2}\partial_x T)$ for this case yields the self-similar solution $T(x,t) = T_0(1 - x/x_f)^{0.39}$, $x_f = 1.045 a^{2/9}(I/c_v)^{5/9} t^{7/9}$, $T_0 = 1.33 a^{-2/9}(I/c_v)^{4/9} t^{2/9}$ (the numerical coefficients are fits to the numerical solution). From the pressure equilibrium $nkT_0 = p_L$ the time t_0 is obtained at which hole boring stops, $t_0 = 1.7\, a(I/c_v)^{5/2} c^{-9/2} \sim \rho^{-7/2} I^{5/2}$; ($\mathcal{R} = 0$). For $\rho = 0.5$ g cm^{-3} and $I = 10^{20}$ W cm^{-2}, one obtains $t_0 = 14$ ps, i.e., matter perforation comes to an end even before the available time of 30 ps has passed. For $t > t_o$ the critical surface moves back into the corona.

In conclusion, in coronal ignition, hole boring does not constitute an essential element. The critical surface, and hence the region of laser pulse absorption, can hardly be brought close to the dense core; on the contrary, it remains in a peripheral zone of the compressed pellet. Furthermore, if one takes into account that there is also a lateral shock wave which travels faster in the less dense peripheral regions ($v_S \sim \rho_0^{-1/2}$), one realizes that deep hole boring would result in the formation of a large crater and the disassembly of the precompressed pellet, rather than end up with an elongated narrow channel.

The studies of coronal fast ignition without hole boring show that the scheme we propose works. Diffusive energy transport leads to ignition energies as low as 10 kJ. There are indications that in a more sophisticated design this limit may perhaps be brought down to 3–5 kJ, if ballistic transport in the highly compressed core is absent. As binary collision estimates show, there is a good chance for diffusive transport much beyond solid density [19]. Coronal ignition offers several advantages in comparison to the standard scheme with central spark ignition: (i) decoupling of compression from ignition, leading to further relaxed constraints on Rayleigh-Taylor growth compared with [1], (ii) burn fractions as high as in central spark ignition (or perhaps higher), (iii) drastic lowering of symmetry constraints in pellet compression without sensitive reduction of burn fractions, (iv) no tailoring of the ignitor pulse required owing to absence of hole boring. Property (iii) may have a larger impact on future pellet design (perhaps already on NIF [20] and LMJ [21]) and on the decision direct vs indirect drive. It seems that in ICF, when considering the energy losses by indirect drive and its technical complications in a reactor design against the release of symmetry requirements in coronal ignition, direct drive is highly favored again.

This work has been supported by the European Commission through the TMR Network SILASI (Super Intense LAser pulse-Solid Interaction), No. ERBFMRX-CT96-0043.

[1] M. Tabak *et al.,* Phys. Plasmas **1**, 1626 (1994).
[2] J. Nuckolls *et al.,* Nature (London) **239**, 129 (1972).
[3] J. Lindl, Phys. Plasmas **2**, 3933 (1995).
[4] S. Atzeni, in *Inertial Fusion Sciences and Applications,* edited by Ch. Labaune, W. J. Hogan, and K. A. Tanaka (Elsevier, Paris, 2000), p. 415.
[5] A. Pukhov and J. Meyer-ter-Vehn, in *Laser Interaction and Related Plasma Phenomena,* edited by Sadao Nakai and G. M. Miley, AIP Conf. Proc. No. 369, (AIP, New York, 1996) p. 213.
[6] K. A. Tanaka *et al.,* in *Inertial Fusion Sciences and Applications* (Ref. [4]), p. 401 (see also Refs. [4,6,7] therein).
[7] H. Ruhl, A. Macchi, P. Mulser, F. Cornolti, and S. Hain, Phys. Rev. Lett. **82**, 2095 (1999).
[8] T. Yabe *et al.,* Comput. Phys. Commun. **66**, 233 (1991); R. Tanaka, T. Nakamura, and T. Yabe, Comput. Phys. Commun. **126**, 232 (2000).
[9] S. Atzeni, A. Caruso, and V. A. Pais, Nuovo Cimento **64**, 383 (1981).
[10] S. Hain, P. Mulser, F. Cornolti, and H. Opower, Laser Part. Beams **17**, 245 (1999).
[11] S. Hain, *Propagation of Intense Laser Radiation in Matter,* (GCA-Verlag, Herdecke, 1999), p. 88 (in German).
[12] A. R. Bell, J. R. Davies, S. M. Guérin, and H. Ruhl, Plasma Phys. Controlled Fusion **39**, 653 (1997); J. R. Davies, A. R. Bell, M. G. Haines, and S. Guérin, Phys. Rev. E **56**, 7193 (1997).
[13] M. Tatarakis *et al.,* Phys. Rev. Lett. **81**, 999 (1998); M. Borghesi *et al.,* Phys. Rev. Lett. **83**, 4309 (1999); *Inertial Fusion Sciences and Applications* (Ref. [4]), p. 974; L. Gremillet, *et al., Inertial Fusion Sciences and Applications* (Ref. [4]), p. 451.
[14] H. Ruhl, Rev. Mod. Phys. (to be published).
[15] A. Pukhov and J. Meyer-ter-Vehn, Phys. Rev. Lett. **79**, 2686 (1997).
[16] J. C. Adam, A. Héron, S. Guérin, G. Laval, P. Mora, and B. Quesnel, Phys. Rev. Lett. **78**, 4765 (1997); B. F. Lasinski *et al.,* Phys. Plasmas **6**, 2041 (1999); R. J. Mason and M. Tabak, Phys. Rev. Lett. **80**, 524 (1998).
[17] J. Meyer-ter-Vehn, Nucl. Fusion **22**, 561 (1982).
[18] P. Mulser, S. Hain, and F. Cornolti, Nucl. Instrum. Methods Phys. Res., Sect. A **415**, 165 (1998).
[19] C. Deutsch *et al.,* Phys. Rev. Lett. **77**, 2483 (1996).
[20] E. M. Campbell and W. J. Hogan, in *Inertial Fusion Sciences and Applications* (Ref. [4]), p. 9.
[21] L. M. André, in *Inertial Fusion Sciences and Applications* (Ref. [4]), p. 32.